Automotive Experiences
Vol. 7 No. 2 (2024) pp. 252-269
p-ISSN: 2615-6202 e-ISSN: 2615-6636

Research Paper

Modeling of a PEM Fuel Cell Electric Bus with MATLAB/Simulink

John Evans Dakurah[1], **Hamit Solmaz**[1], **Tolga Kocakulak**[2]

[1]Department of Automotive Engineering, Gazi University, Ankara, 06560, Turkey
[2]High School of Technical Sciences, Burdur Mehmet Akif Ersoy University, Burdur, 15030, Turkey

johnevansdakurah@gmail.com (J.E.D), hsolmaz@gazi.edu.tr (H.S)

https://doi.org/10.31603/ae.11471

Published by Automotive Laboratory of Universitas Muhammadiyah Magelang

Article Info
Submitted:
31/05/2024
Revised:
11/07/2024
Accepted:
25/07/2024
Online first:
18/09/2024

Abstract

There have been great strides in recent years in the shift from conventional Internal Combustion Engine Vehicles (ICEVs) because of the deteriorating effects the fossil fuels they use have on the environment. Although lithium-ion battery electric vehicles (EVs) address some of these environmental problems, they do not appear to be a promising alternative because of their limited range, long charging duration, and the negative effects resulting from the production and disposal of their batteries. Demand for hydrogen vehicles has therefore increased over the years. This is because, since they use hydrogen as a fuel, they offer longer ranges, shorter refueling durations, and zero emissions. In this paper, a 70 kW PEM Fuel Cell Electric Bus (PEMFCEB) which has a 50 kWh buffer battery, and a total hydrogen capacity of 38 kg is modeled using MATLAB/Simulink. In the study, two hybrid energy management systems – fuzzy logic and conventional on-off using a 'Relay' block – are integrated into the model. By simulating several repeated NEDC (New European Driving Cycle) and WLTP (Worldwide Harmonized Light Vehicle Test Procedure) cycles, the overall performance of the bus including its total range, consumption of hydrogen and oxygen, and fuel cell efficiency under each energy management system is analyzed and compared. For instance, during the NEDC cycle, the bus achieves a total range of 492.02 km with Fuzzy Logic compared to 448.85 km with the traditional on-off system. Similarly, under the WLTP cycle, the bus exhibits a total range of 407.61 km and 362.33 km with Fuzzy Logic and on-off techniques respectively.

Keywords: Electric vehicle; Hydrogen vehicle; Matlab/Simulink; Modeling; PEM fuel cell; Simulation

1. Introduction

The urgency for more eco-friendly and cleaner options to internal combustion engine vehicles and lithium-ion battery powered electric vehicles underlines the necessity of PEM Fuel Cell Electric Vehicles (PEMFCEVs), which use hydrogen as a fuel to generate power, giving out solely water vapor and heat. They are easy and fast to refuel and cover relatively longer ranges [1]–[6].

Internal combustion engine vehicles (ICEVs) burn fuels such as gasoline and diesel in order to produce needed power for propulsion. This results in the release of several harmful emissions such as carbon dioxide (CO_2), carbon monoxide (CO), nitrogen oxides (NOx) and particulate matter (PM) which can have detrimental effects on both the environment and the health of living things including humans [7], [8].

Compared to ICEVs, electric vehicles (EVs) are much cleaner because they do not produce tailpipe emissions. However, the processes involved in the production of lithium-ion batteries, which EVs require, contribute significantly to increasing carbon footprint [9]. Moreover, EVs have limited ranges and can require considerable amount of time to charge [10]. Based on this, EVs do not appear to be replacing ICEVs any time soon.

PEMFCEVs address most of the drawbacks that both ICEVs and EVs come with. First, they are powered by hydrogen which can be obtained from renewable sources [1]. The hydrogen reacts

with oxygen in a fuel cell with no emissions [6]. Plus, PEMFCEVs have long ranges with quick and easy refueling features [11].

Several studies have been conducted on the modeling of PEM Fuel cells and electric vehicles. Schaltz designed and modeled an electric vehicle. He found that the vehicle consumed 148.3 Wh/km energy over 14 NEDC drive cycles [12]. Kiyakli and Solmaz also developed a model of an Electric Vehicle using MATLAB/Simulink. Their results showed that under the NEDC drive cycle the vehicle had a range of 177.7 km with an energy consumption of 13.8 kWh/100 km when compared to the WLTP cycle where it has a range of 157.7 km with an energy consumption of 15.49 kWh/100 km [13]. Likewise, Thallapalli, Kıyaklı, and Kocakulak created a model of an electric tractor so they could calculate the amount of energy consumed under different duties. The results from their study showed that when the reduction ratio was 50 the rotary harrow, atomizer, and shredder duties consumed 3.985 kWh, 1.266 kWh, and 3.787 kWh energy respectively. Results also showed that when the reduction ratio was increased to 100, the energy consumption in the rotary harrow, atomizer, and shredder duties decreased by 9.56%, 9.55%, and 6.65% respectively [14]. Similarly, Karakaş, Şeker, and Solmaz developed a model of an electric bus using MATLAB/Simulink in order to ascertain how much money could be saved on a real urban bus route. They found that the bus had a total range of 335.2 km when the battery was fully charged, and that it consumed 73.09 kWh over 100 km. They also found that the electric bus was more economical relative to diesel and CNG buses over a 100 km distance [15]. Furthermore, Hemi, Ghouili, and Cheriti implemented a fuzzy logic power control mechanism for a fuel cell powered vehicle under different power source configurations. Their results indicated that the amount of hydrogen consumed was less in the FC (Fuel Cell)/B (Battery) and FC (Fuel Cell)/B (Battery)/SC (Super Capacitor) setup than in the FC/SC setup. They also showed that the FC/B/SC combination improved the longevity of the battery by allowing fast charging and draining [16]. Additionally, Mebarki, T. Rekioua, Mokrani, D. Rekioua, and Bacha modeled a PEM fuel cell and battery hybrid system using MATLAB/Simulink where they demonstrate the practicality of this system when applied in an electric vehicle [17].

Despite the extensive research into electric vehicles and fuel cell technologies, there still remains a significant gap in the application of PEM fuel cells in electric vehicles especially the massive role hybrid energy management systems play in the overall performance of the vehicle. In this study, therefore, a comprehensive model of a PEM Fuel Cell Electric Bus (PEMFCEB) with two hybrid energy management systems is presented using MATLAB/Simulink.

2. Method

Fuel cell electric vehicles combine the features of a typical electric vehicle and a fuel cell stack into one system. This section is thus divided into three sub sections including the modeling of an Electric Drive System and Vehicle Dynamics, the modeling of a Fuel Cell Stack and the modeling of Hybrid Energy Management systems.

2.1. Electric Drive System and Vehicle Dynamics Model

2.1.1. Electric Motor Model

Fuel cell buses rely on electric motors to convert electrical energy from fuel cells and battery packs into mechanical energy so as to move the vehicle. In this study, the speed-torque values of an electric motor "SUMO HD HV3500" were used for the electric motor model. The features of this electric motor are given in **Table 1** and its speed-torque curve is shown in **Figure 1**.

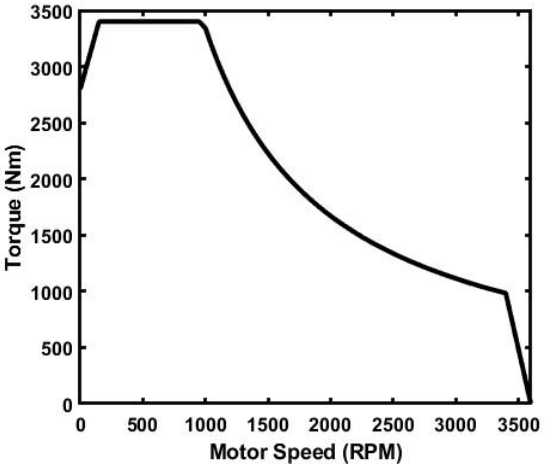

Figure 1. Electric motor speed-torque curve

Table 1. Characteristics of SUMO HD HV3500 electric motor [18]

Feature	Value
Inverter	CO300-HV
Peak power (kW)	370
Continuous power (kW)	260
Operating speed (RPM)	0-3400
Continuous torque (NM)	1970
Peak torque (NM)	3445
Mass (kg)	376

In the Simulink model of the electric motor, the torque and speed values of the motor were put into a "1-D Lookup Table". The lookup table determines the motor torque according to the angular velocity of the vehicle which it takes as an input. The output is the motor torque at that given angular velocity. In this study, the electric motor is assumed to be 90% efficient. **Figure 2** shows the Simulink model of the electric motor.

2.1.2. Vehicle Resistance Forces Model

Fuel cell electric buses like other vehicles encounter resistance during motion. These resistance forces retard motion increasing the consumption of hydrogen and thus reducing the overall range of the vehicle. Vehicles generally encounter four different resistance forces during motion. These include aerodynamic or air resistance, tire rolling resistance, acceleration resistance and gradient resistance forces [19], [20]. **Figure 3** shows the resistance forces acting on a bus.

Aerodynamic resistance force also known as air or drag resistance counteracts the movement of the vehicle as it goes through air. This usually results from the interaction of the vehicle with air molecules as it moves through the air. Aerodynamic resistance force usually becomes pronounced at very high velocities. The expression for calculating aerodynamic resistance force is given by Eq. (1) [14], [21].

$$F_d = \frac{\rho C_d A_f (V \pm V_o)^2}{2} \quad (1)$$

Tire rolling resistance force acts on the wheels of a vehicle as it rolls over the road surface. This force depends on factors like the tire construction, tread design, and the type of road. The formula for calculating this force is given by Eq. (2) [19], [21]:

$$F_{roll} = \text{mg}C_{rr}cos\theta \quad (2)$$

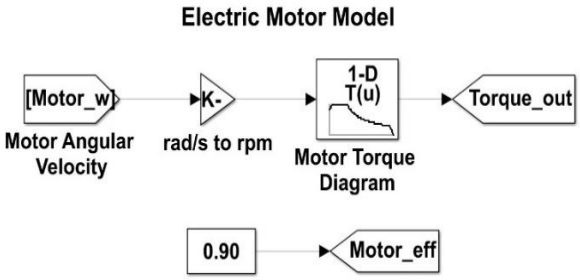

Figure 2. Simulink model of electric motor

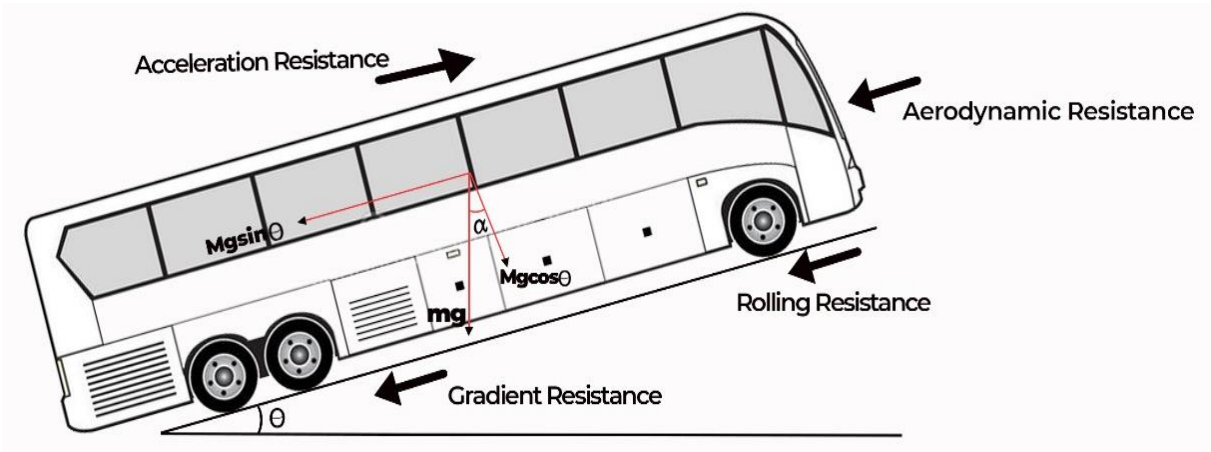

Figure 3. Resistance forces acting on a bus

A vehicle accelerating or decelerating often experiences a resistance force in an opposite direction. This force is known as acceleration force and is the product of the mass and acceleration of the vehicle as shown in Eq. (3) [21].

$$F_{acc} = \text{ma} \tag{3}$$

Gradient resistance is a type of force that acts on the vehicle when it is moving up or down a hill on a slope. This force is given by Eq. (4) [21].

$$F_g = \text{m g } sin\theta \tag{4}$$

The total retarding force on the vehicle is given by the sum of the aerodynamic, tire rolling, acceleration and gradient resistance forces as shown in Eq. (5) [14].

$$F_{total} = F_d + F_{roll} + F_{acc} + F_g \tag{5}$$

The resistance torque due to the total resistance force is equally calculated as a product of the total resistance force and radius of the wheel as shown in Eq. (6).

$$T_{resis} = F_{total}\, x\, r_w \tag{6}$$

Figure 4 shows a Simulink model of the total resistive torque which acts on the vehicle. In the model, the resistance torque due to the resistance forces and the brake torque give the total resistance torque acting on the vehicle.

2.1.3. *Driving Cycles*

Driving cycles are a set of data points that show the speed of a vehicle against time. They are helpful in measuring different vehicle performance metrics such as fuel consumption and exhaust gas emissions. In order to compare the performance of the model under different conditions, two driving cycles are used in this study: NEDC (New European Driving Cycle) and WLTP (Worldwide Harmonized Light Vehicles Test Procedure). The NEDC driving cycle is made up of two main sections: four repeating Urban Driving Cycle (UDC) which last for 780 seconds and one Extra-Urban Driving Cycle (EUDC) which lasts for 400 seconds. The WLTP driving cycle on the other hand is made up of four sections: low, medium, high, and extra-high speed phases with the entire cycle spanning 1800 seconds. The features of these driving cycles are summarized in **Table 2** and their speed profiles are given in **Figure 5** and **Figure 6**.

Table 2. Features of NEDC and WLTP drive cycles

Feature	NEDC	WLTP
Time (s)	1180	1800
Average speed (km/h)	33.63	46.50
Maximum speed (km/h)	120	131
Total distance (km)	11.02	23.25

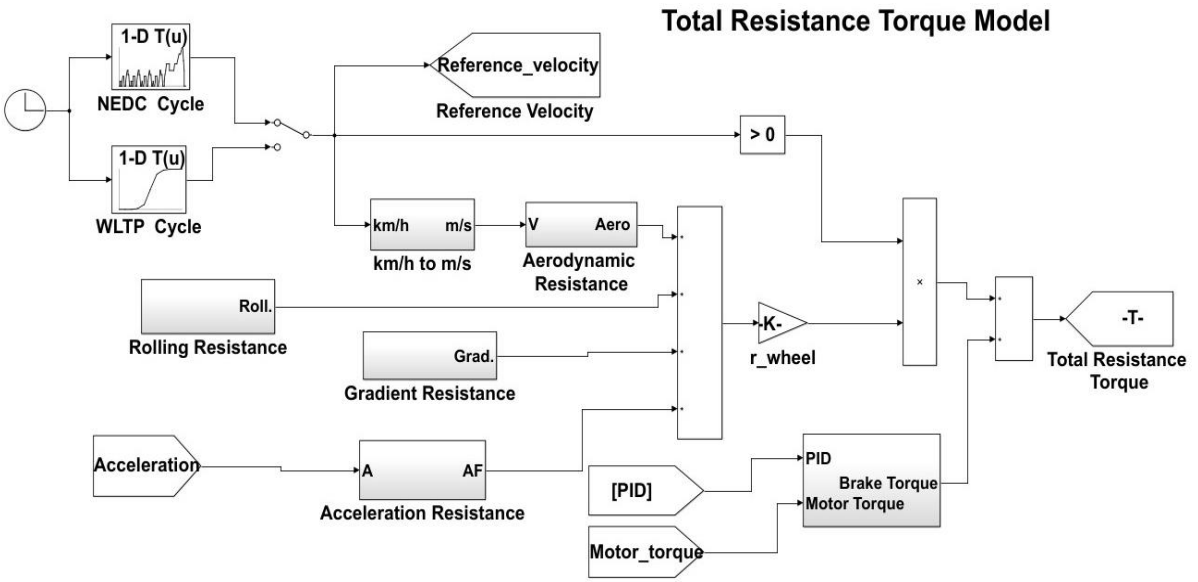

Figure 4. Total resistance forces and torque model

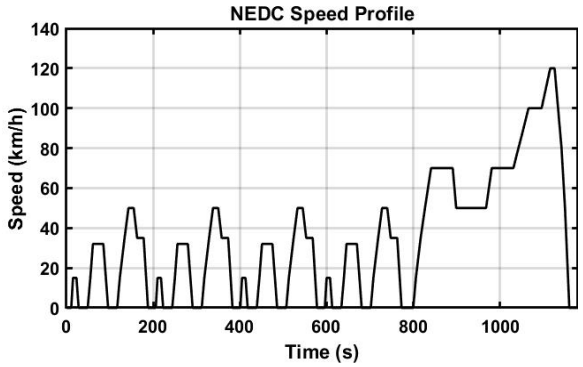

Figure 5. NEDC speed profile

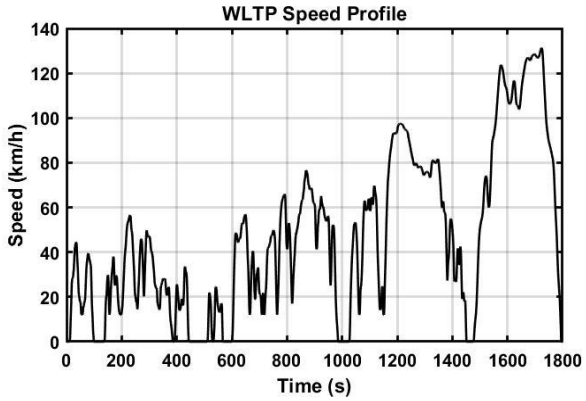

Figure 6. WLTP speed profile

2.1.4. *PID Speed Controller Model*

This section shows the implementation of a speed controller model that equates the velocity of the bus to the reference drive cycle velocities – NEDC and WLTP. To do this, a PID controller block was used. The block which takes the reference and vehicle velocities as inputs, outputs values between "-1" and "1". Values between "0" and "1" indicate the accelerator pedal position whereas those between "-1" and "0" indicate the brake pedal position. The Ziegler-Nichols approach was used to determine the values of the parameters within the PID block. The integral (I) and derivative (D) values were kept at 0 while the proportional value (P) was increased. Afterward, the "PID Tuner" was used to modify the values of the parameters. **Figure 7** illustrates the PID controller model.

2.1.5. *Vehicle Powertrain System Model*

To obtain a vehicle dynamics model within Simulink, a "transfer function" of the powertrain system must first be determined. As seen in **Figure 8**, a fuel cell stack, battery pack and an electric motor make up the powertrain of a typical fuel cell vehicle.

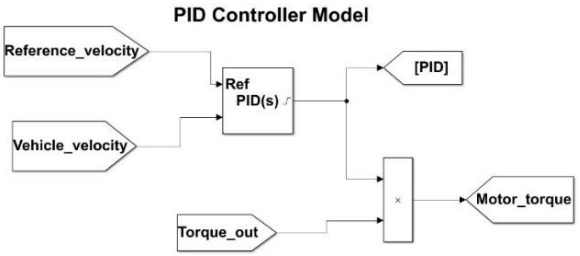

Figure 7. PID controller model

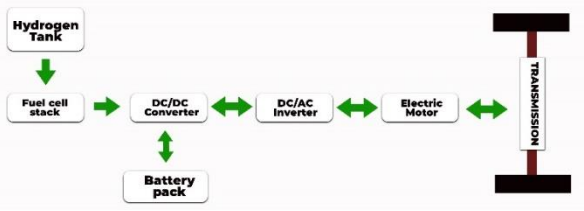

Figure 8. Powertrain system diagram of a typical FCEV

The "transfer function" of a powertrain system – which relates the angular acceleration to the torque and the shaft's moment of inertia – is shown in Eq. (7) [13], [22]–[24].

$$\frac{d\omega}{dt} = \frac{M_{net}}{j_{total}} \tag{7}$$

By simplifying Eq. (7) the velocity of the motor is obtained as shown in the following equations.

$$d\omega = \frac{M_{net}}{j_{total}} dt \tag{8}$$

$$\omega = \int \frac{M_{net}}{j_{total}} dt \tag{9}$$

$$\omega = \int \left(\frac{M_{motor}\, x\, \eta_{motor} - M_{resis}\, x\, \frac{\eta_{diff}}{i_{diff}}}{\frac{6\, x\, J_{wheel} + 2\, x\, J_{axle}}{(i_{diff})^2\, x\, \eta_{diff}}} \right) \tag{10}$$

The angular velocity of the motor obtained in Equation 10 was divided by the efficiency of the differential and the result was multiplied by the wheel's radius to determine the vehicle velocity. The derivative and integral of the velocity equally give the acceleration and total distance traveled by the vehicle respectively as illustrated in **Figure 9**.

2.1.6. *Regenerative Braking Model*

Electric and hydrogen vehicles undergo a mechanism called Regenerative Braking. During this mechanism, their electric motors convert kinetic energy to electrical energy and store it for

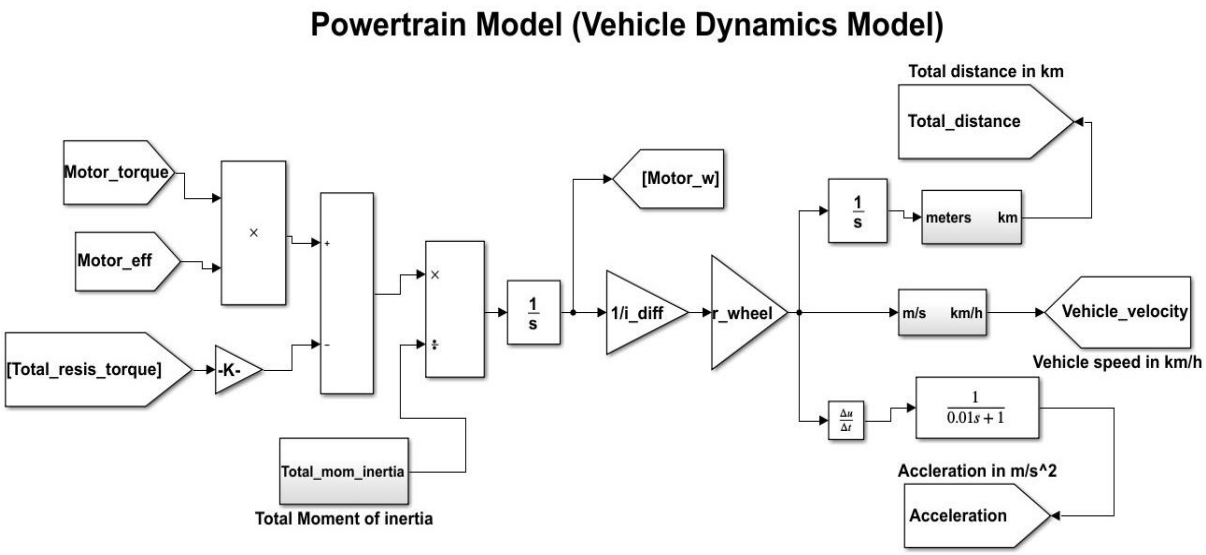

Figure 9. Vehicle powertrain and dynamics model

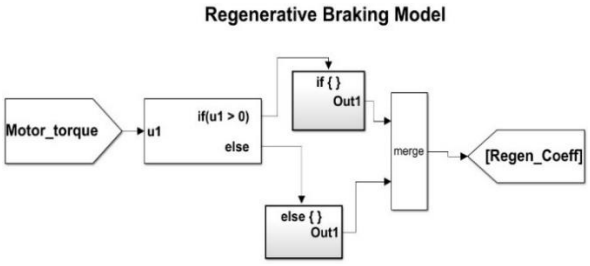

Figure 10. Regenerative braking model

later use. This improves the overall efficiency and driving range of the vehicle [25]. In this model, regenerative braking was integrated with a brake gain of 30%. **Figure 10** shows the regenerative braking model.

2.2. *Fuel Cell Stack Model*

2.2.1. *PEM Fuel Cell Electrochemical Model*

This section presents an electrochemical-based model of the PEM fuel cell. This model introduced by Corrêa, Farret, Canha, and Simões [26], has been used in many studies. In this paper also, it is used to model the fuel cell stack. Eq. 11 provides the overall output voltage V_{Stack} of a PEM cell stack which has a total of N cells.

$$V_{Stack} = N(E_{Nerst} - V_{act} - V_{ohmic} - V_{con}) \quad (11)$$

Where E_{Nernst} represents the reversible potential of each cell and is obtained using the expression (Eq. (12)).

V_{act} is the drop in voltage resulting from the activation between the electrodes of the cathode and anode. It is given by the expression (Eq. (13)).

V_{ohmic} is the loss in voltage resulting from the flow of protons and electrons and is expressed as (Eq. (14)).

V_{con} is the drop in voltage when there is a fall in hydrogen and oxygen concentrations and can be calculated as (Eq. (15)).

C_{O_2} in Eq. (13) and Rm in Eq. (14) can be calculated as Eq. (16) and Eq. (17).

ρ_m in Eq. (17) can be calculated as Eq. (18).

$$E_{Nerst} = 1.229 - 8.5x10^{-4}.(T - 298.15) + 4.3085x10^{-5}.T\left[\ln(P_{H_2}) + \frac{1}{2}\ln(P_{O_2})\right] \quad (12)$$

$$V_{act} = -\left[\xi_1 + \xi_2 T + \xi_3 T.\ln(C_{O_2}) + \xi_4 T.\ln(i_{FC})\right] \quad (13)$$

$$V_{ohmic} = i_{FC}.(R_m + R_c) \quad (14)$$

$$V_{con} = -B.\ln\left(\frac{J}{J_{max}}\right) \quad (15)$$

$$C_{O_2} = \frac{P_{O_2}}{\left[5.08\ x\ 10^6.e^{-\left(\frac{498}{T}\right)}\right]} \quad (16)$$

$$R_m = \rho_m . \frac{l}{A} \tag{17}$$

$$\rho_m = \frac{181.6\left[1 + 0.03\left(\frac{i_{FC}}{A}\right) + 0.062\left(\frac{T}{303}\right)^2 . \left(\frac{i_{FC}}{A}\right)^{2.5}\right]}{\left[\psi - 0.634 - 3.\left(\frac{i_{FC}}{A}\right) x\ exp.\left[4.18\ .\left(\frac{T-303}{T}\right)\right]\right]} \tag{18}$$

The mathematical model of the PEM fuel cell requires that some parameters be set. **Table 3** shows the base parameter values based on literature data [27]–[29] and some adjustments that were made to meet the needs of the model.

After running the mathematical model of the PEM fuel cell in MATLAB, a Current Density – Voltage curve was obtained as shown in **Figure 11**.

To find the power (P_{FC}), current (i_{FC}) was multiplied by cell voltage (V_{Stack}) [30]–[32].

$$P_{FC} = i_{FC} . V_{Stack} \tag{19}$$

Figure 12 shows the fuel cell power density curve.

To obtain the instantaneous fuel cell power generation model in Simulink, the current and power density values of the cell were put into a '1-D Lookup Table'. The total power generated by the cell is calculated by multiplying the power density by the cell area and number of cells. The power produced was integrated over time to give the energy (kWh) of the cell as shown in Equation 20. In this study, each fuel cell has a total area of 250 cm², and the entire stack comprises of a total of 300 cells. This configuration was chosen so as to achieve a maximum power output of approximately 70 kW.

Figure 13 shows the instantaneous power generation model of the fuel cell in Simulink.

$$E = \int \frac{\left(P_{density} . A . N\right)}{1000} \tag{20}$$

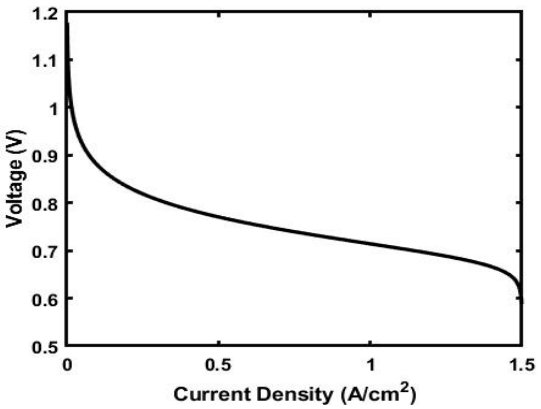

Figure 11. Curve of current density – voltage

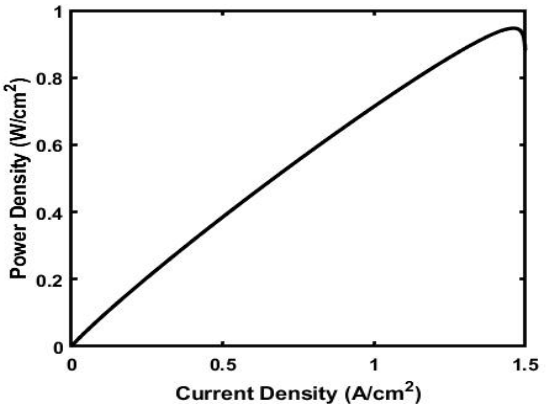

Figure 12. Curve of current density – power density

Table 3. Fuel cell parameters and simulation data

Parameter	Value	Adjusted Value
T	333 K	333 k
P_{H2}	1.0 atm	5 atm
P_{O2}	0.2095 atm	3.5 atm
ξ_1	-0.948	-0.948
ξ_2	0.00286+0.0002•log(Acell)+(4.3•10^{-5}• (log(CH2)))	0.00286+0.0002•log(Acell)+(4.3•10^{-5}• (log(CH2)))
ξ_3	7.6×10^{-5}	7.6×10^{-5}
ξ_4	-1.93•10^{-4}	-1.93•10^{-4}
J_n	3 mA/cm^2	3 mA/cm²
J_{max}	469 mA/cm²	1.50 A/cm²
R_c	0.0003 Ω	0.0003 Ω
B	0.016 V	0.016 V
ψ	23	23

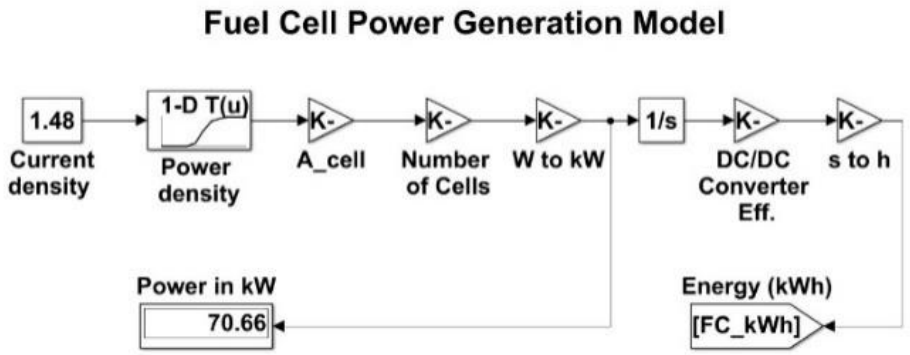

Figure 13. Power generation model of fuel cell

2.2.2. *Fuel Cell Efficiency Model*

PEM Fuel Cells have electrical efficiencies generally ranging between 40-60% [33]. The formula for calculating the efficiency of a fuel cell is given in Eq. (21) [31], [34].

$$\eta_{FC} = \frac{N \,.F\,.V_{stack}}{\Delta H} x\ 100 \qquad (21)$$

Figure 14 gives the Simulink model of the efficiency of the fuel cell using Eq. (21). In the figure, for example, the cell is 49.53% efficient at 0.80 A/cm^2.

2.3. *Energy Management Systems Model*

Choosing the right energy management technique for the bus is very important because it can optimize the efficiency and operation of the fuel cell allowing the bus to reach longer ranges. In this paper, two of such techniques – fuzzy logic and conventional one-off – are used.

2.3.1. *Energy Control with Fuzzy Logic Technique*

Fuzzy Logic is a common energy management system. It is a way of dealing with uncertainty by using linguistic variables to mimic the way humans think [35]. To do this, input data sets and their membership functions are often defined and put into "if-else" statements to obtain output variables [36]–[39]. In the Simulink model of the fuzzy logic controller, there are two input variables and one output variable. The power demand (Power_demand) of the bus and the State of Charge (SOC) of the battery were set as the input variables, while the current density (Current_density) of the fuel cell was set as the output variable. Using the MATLAB 'Fuzzy Logic Designer' toolbox a design of the Fuzzy Logic technique was obtained as shown in **Figure 15**.

The membership functions of the "Power_demand" input variable were configured as very low (VL), low (L), moderately low (ML), moderate (M), moderately high (MH), high (H), very high (VH), and extremely high (EH) as shown in **Figure 16**.

Similarly, the "SOC" input variable membership functions were configured as very low (VL), low (L), medium (M), high (H), and very high (VH) as illustrated in **Figure 17**.

In a similar fashion, the membership functions for the "Current_density" output variable were set as very low (VL), low (L), moderately low (ML), low to medium (L2M), medium (M), medium to high (M2H), high (H), very high (VH), and extremely high (EH) as shown in **Figure 18**.

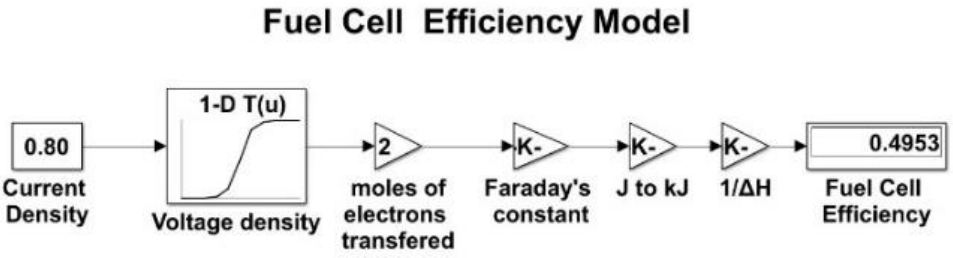

Figure 14. Simulink model of fuel cell efficiency

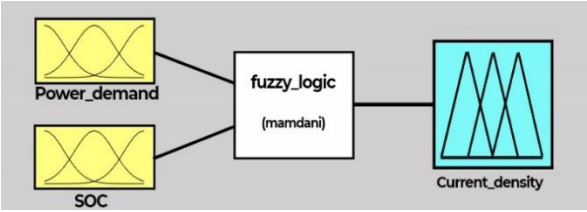

Figure 15. Matlab design of fuzzy logic technique

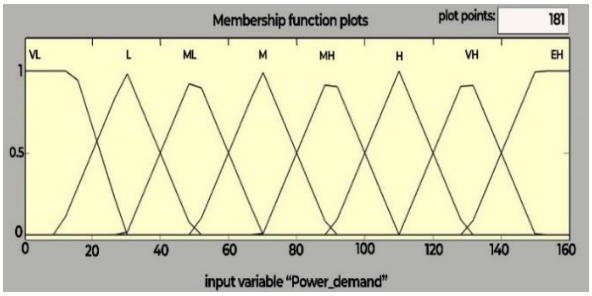

Figure 16. Membership functions for power demand input variable

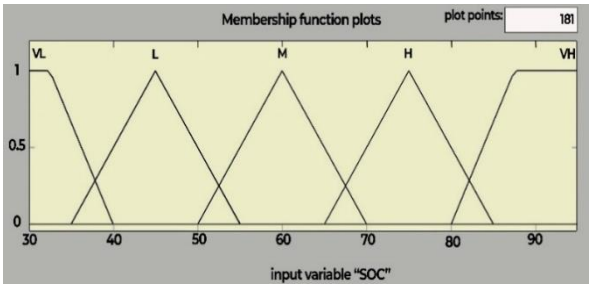

Figure 17. Membership functions for SOC input variable

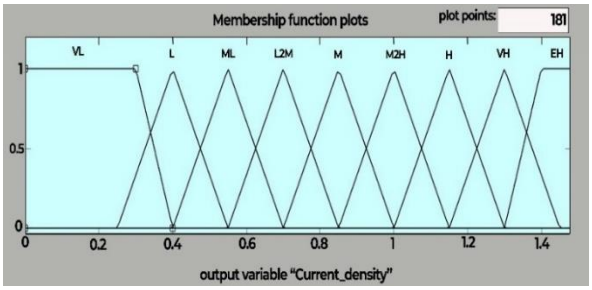

Figure 18. Membership functions for current density output variable

In all, a total of 40 fuzzy logic rules were formulated as seen in **Table 4**.

In summary, the fuzzy logic determines the current density taking into account the power need and the SOC. If the power need is high and the SOC of the battery is low, for instance, the fuel cell will raise its power production to meet the demands of the vehicle and also recharge the battery. Conversely, if the SOC is high and the power need is low, the fuel cell reduces its power production while the battery meets most of the power demands. **Figure 19** gives the Simulink model of the Fuzzy Logic energy management strategy.

2.3.2. *Energy Control with Traditional On-Off Technique*

Under this simple energy management technique, a 'Relay' block is used to switch the current density between two values depending on only the value of the SOC. The Simulink model of this technique is shown in **Figure 20**.

In this model, the fuel cell was made to operate at a current density of 0.50 A/cm² till the SOC of the battery falls below 30%. Whenever this happens, the current density switches to 1.20 A/cm² until the SOC reaches 90% where the current density switches again to 0.50 A/cm².

2.3.3. *State of Charge (SOC) Model*

Having implemented the two hybrid energy management systems, the Simulink model of the battery SOC is presented in this section. The SOC generally depends on the total energy demand of the vehicle as well as the total energy that the fuel cell produces. Also during regenerative braking, the battery is charged with a gain of 30%. **Figure 21** shows the Simulink model of the power demand of the bus and **Figure 22** gives the overall model of the SOC for the battery.

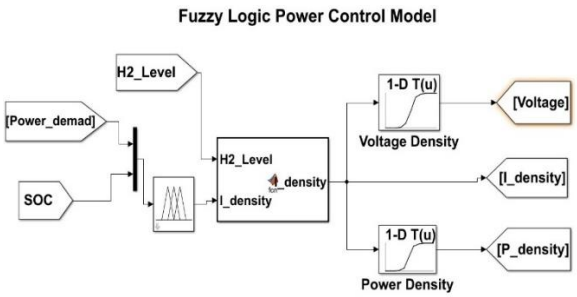

Figure 19. Simulink model of fuzzy logic energy management system

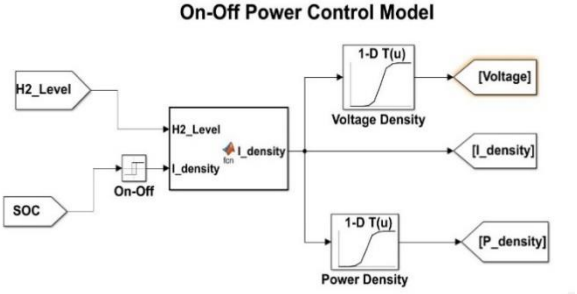

Figure 20. Simulink model of traditional on-off energy management system

Table 4. Fuzzy logic rules

Current Density		SOC				
		VL	L	M	H	VH
Power Demand	VL	L2M	ML	L	VL	VL
	L	M	L2M	ML	L	VL
	ML	M2H	M	L2M	ML	L
	M	H	M2H	M	L2M	ML
	MH	H	H	M2H	M	L2M
	H	VH	H	H	M2H	M
	VH	EH	VH	H	H	M2H
	EH	EH	EH	VH	H	H

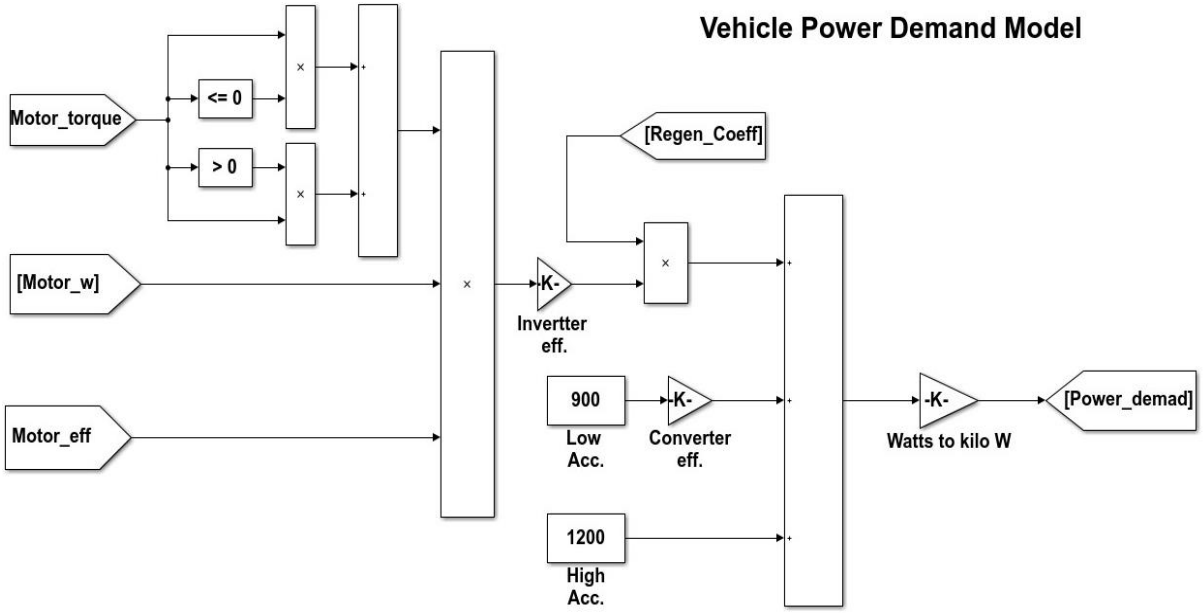

Figure 21. Simulink model of power demand of vehicle

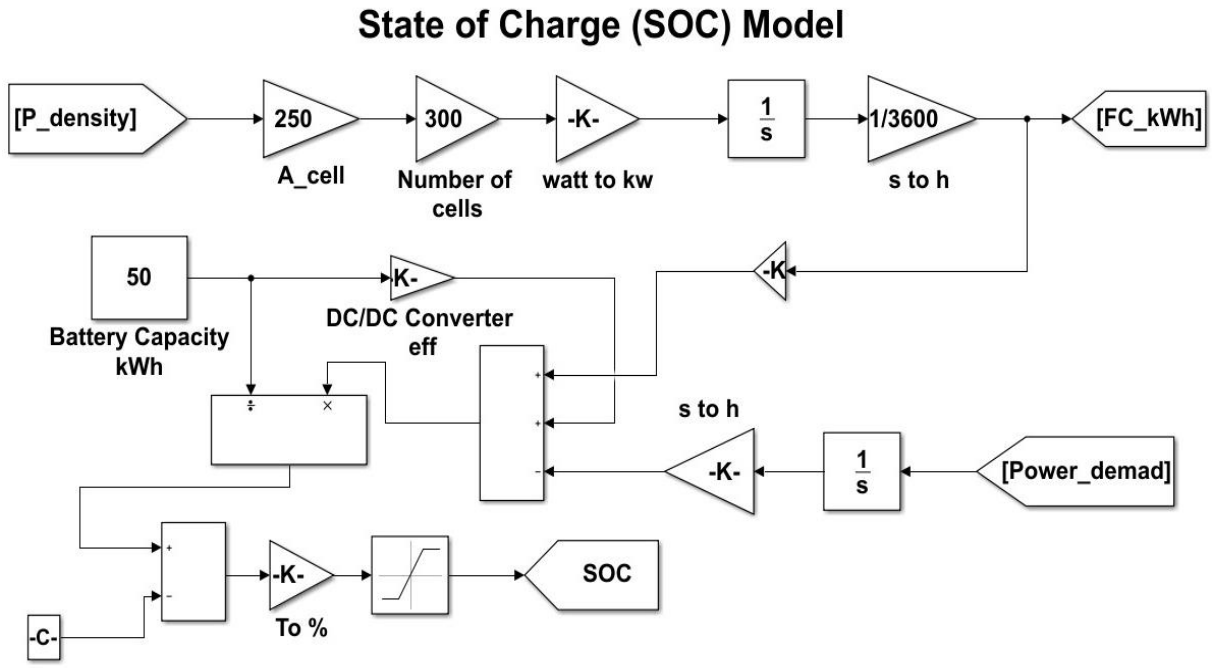

Figure 22. Simulink model of state of charge (SOC)

2.3.4. *Consumption of Hydrogen and Oxygen Model*

The rate of hydrogen consumption in mol/s and in g/s are given by Eq. (22) and Eq. (23) [40], [41].

$$\dot{n}_{H_2} = \left(\frac{i_{FC}}{2F}\right) \tag{22}$$

$$\dot{m}_{H_2} = \left(\frac{i_{FC}}{2F}\right) M_{H_2} \tag{23}$$

From the reaction between hydrogen and oxygen, two moles of hydrogen react with one mole of oxygen to give water as shown in Eq. (24) [30]:

$$2H_2 + O_2 \rightarrow 2H_2O \tag{24}$$

The rate of oxygen consumption can therefore be calculated using the following equations:

$$\dot{n}_{O_2} = \frac{\dot{n}_{H_2}}{2} \tag{25}$$

$$\dot{n}_{O_2} = \frac{i_{FC}}{4F} \tag{26}$$

$$\dot{m}_{H_2} = \left(\frac{i_{FC}}{4F}\right) M_{O_2} \tag{27}$$

The transformations of Eq. (23) and Eq. (27) into Simulink models are given in **Figure 23** and **Figure 24**.

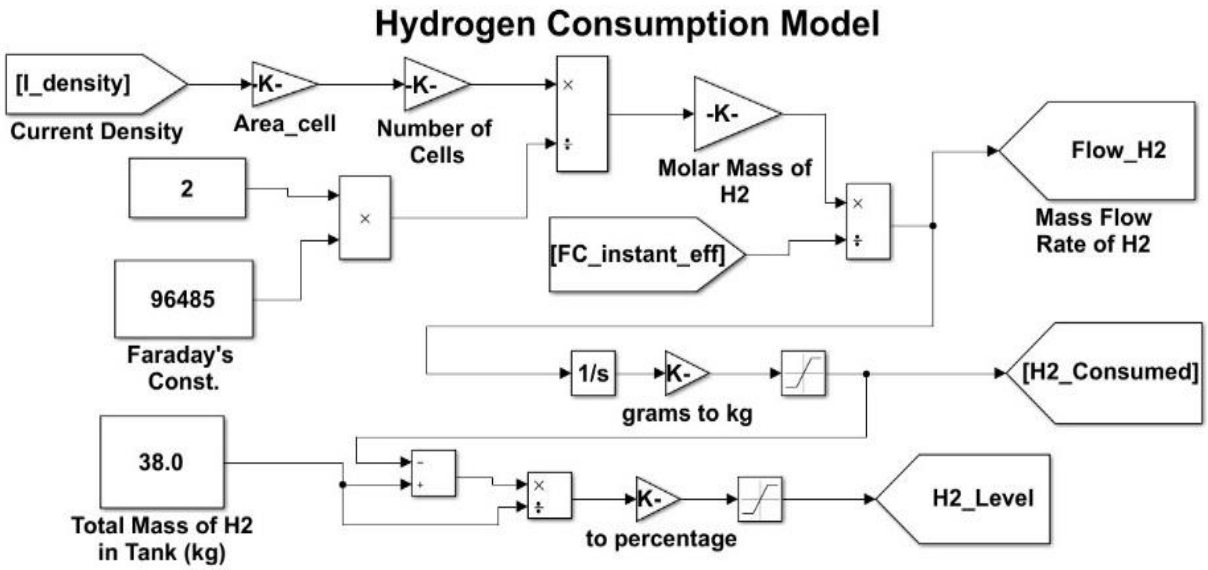

Figure 23. Simulink model of hydrogen consumption

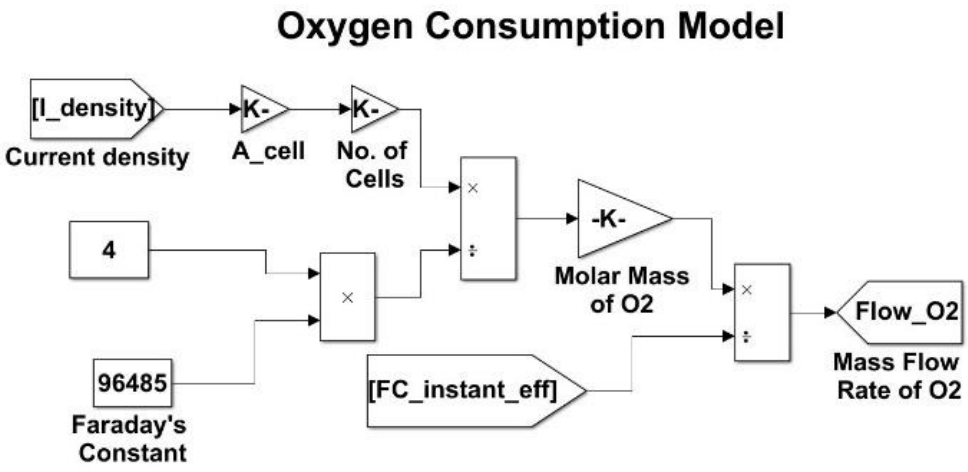

Figure 24. Simulink model of oxygen consumption

3. Results and Discussion

Results from the simulations showed that the velocity of the bus follows the reference drive cycle velocities – NEDC and WLTP. This shows that the PID speed controller model works. Results of the vehicle velocity versus reference drive cycle velocity for each drive cycle are given in **Figure 25**.

Other results from the simulation including vehicle acceleration, motor torque and motor speed for each reference drive cycle are given in the following **Figure 26** to **Figure 28**.

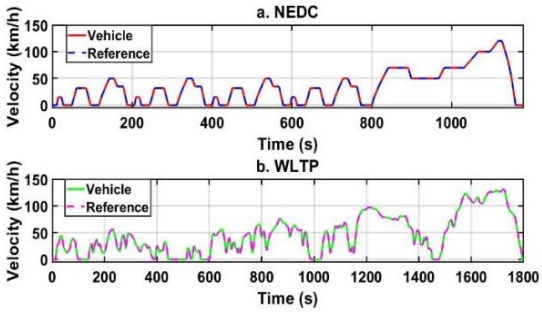

Figure 25. Graph of reference drive cycles versus vehicle velocity (a) NEDC (b) WLTP

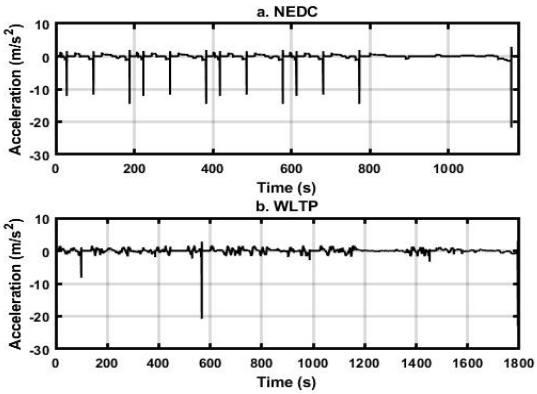

Figure 26. Graph of vehicle acceleration (a) NEDC and (b) WLTP

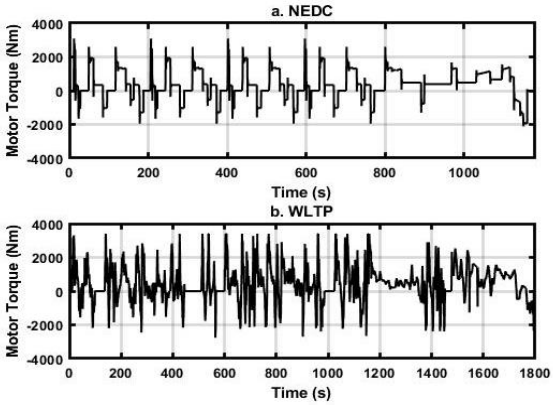

Figure 27. Graph of motor torque (a) NEDC and (b) WLTP

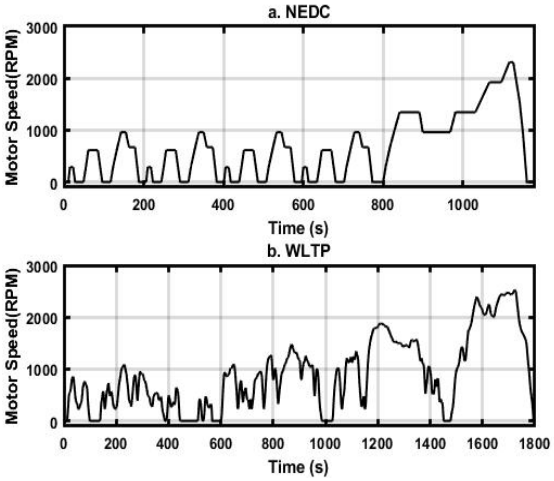

Figure 28. Graph of motor speed (a) NEDC and (b) WLTP

Under the Fuzzy Logic energy management strategy, simulations were carried out for the entire operational range of the bus, that is, close to 45 repeated NEDC cycles corresponding to 492.02 km and over 18 repeated WLTP cycles corresponding to 407.61 km. It was observed that under the NEDC cycle, the bus run on both the fuel cell and the battery for a total of 452.93 km (48631 seconds) until the total hydrogen capacity of 38 kg was depleted. Subsequently, it was observed that the SOC of the battery quickly declined to zero as the battery alone could not sustain the vehicle for an extended range. Similarly, in the WLTP cycle, the hydrogen was entirely consumed after 385.93 km (30167 seconds), leading to a rapid decline of the SOC to zero. The fuel cell exhibited an average efficiency of 52.56% under NEDC, and 50.05% under WLTP. The results of simulations under Fuzzy Logic for both NEDC and WLTP cycles are given in the accompanying **Figure 29** to **Figure 32**.

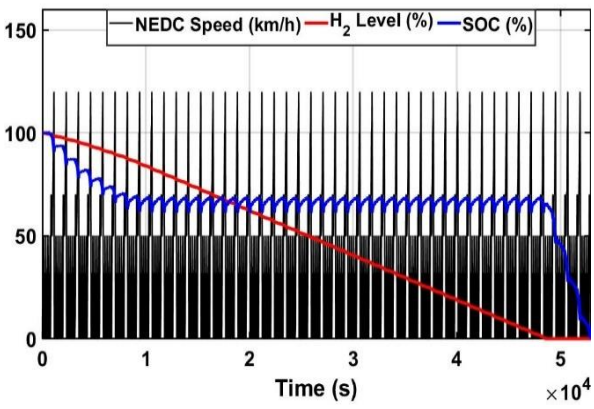

Figure 29. Speed, H_2 level and SOC under fuzzy logic (NEDC)

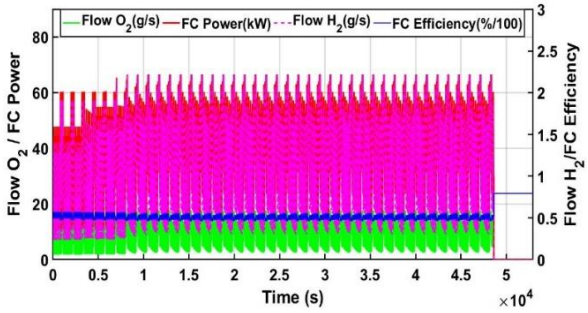

Figure 30. Hydrogen and oxygen flow, fuel cell power and fuel cell efficiency under fuzzy logic (NEDC)

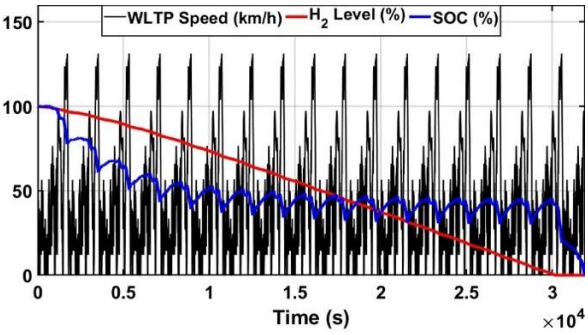

Figure 31. Speed, H2 level and SOC under fuzzy logic (WLTP)

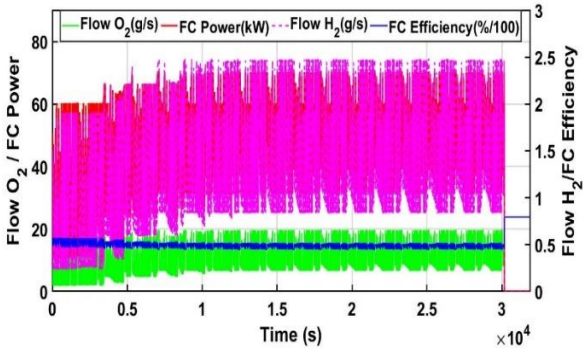

Figure 32. Hydrogen and oxygen flow, fuel cell power and fuel cell efficiency under fuzzy logic (WLTP)

When the energy management strategy was switched to Conventional On-Off, the analysis covered over 41 repeated NEDC cycles, corresponding to a total range of 448.85 km and 16 repeated WLTP cycles corresponding to 362.33 km. During the NEDC cycle, the hydrogen supply was exhausted after 410.67 km (44250 seconds), leading to a sharp decline in the SOC of the battery to zero. Similarly, under the WLTP cycle, the hydrogen supply was depleted after 331.19 km (26052 seconds), again resulting in a quick decline of the SOC to zero. The Fuel Cell was on average 51.55% efficient under NEDC and 49.08% under WLTP. The results of simulations under traditional On-Off for both NEDC and WLTP cycles are given in the accompanying **Figure 33** to **Figure 36**.

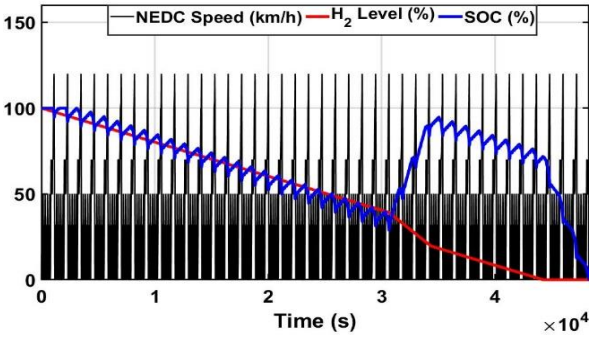

Figure 33. Speed, H2 level and SOC under on-off (NEDC)

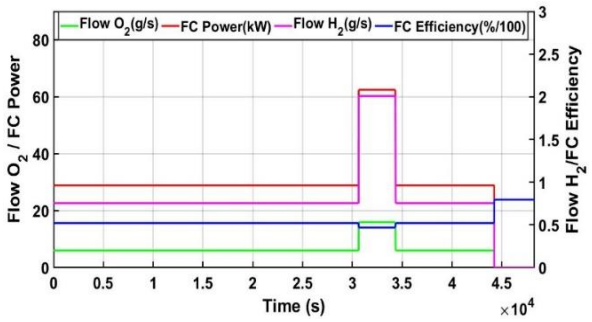

Figure 34. Hydrogen and oxygen flow, fuel cell power and fuel cell efficiency under on-off (NEDC)

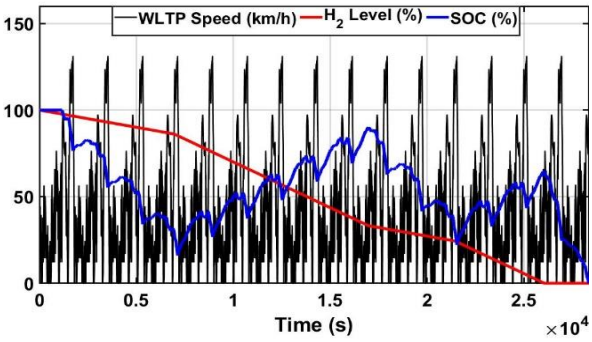

Figure 35. Speed, H2 level and SOC under on-off (WLTP)

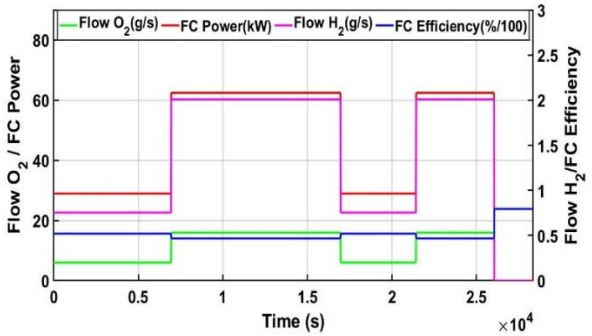

Figure 36. Hydrogen and oxygen flow, fuel cell power and fuel cell efficiency under on-off (WLTP)

In summary, results from the simulation show that the Fuzzy Logic energy management technique increased the range of the bus by 9.62% under NEDC and 12.50% under WLTP cycles when compared to the Conventional On-Off.

In this study, also, simulations were carried out under different vehicle parameters including vehicle mass, aerodynamic drag coefficient and rolling resistance coefficient. Variations in the values of these parameters on hydrogen consumption were examined over one NEDC and WLTP reference drive cycles. The results show that under fuzzy logic an increase in the value of these parameters increased the consumption of hydrogen as compared to the on-off system which maintained a constant rate of hydrogen consumption as a result of being operated between two constant current density values. The results are shown in **Table 5** to **Table 7**.

Similarly, the effects of regenerative braking – when on and off – on the total range of the bus were examined as shown in **Table 8**.

Table 5. Effects of vehicle mass on hydrogen consumption

Vehicle Mass (kg)	Drive Cycle	Energy Technique	Hydrogen Consumed (kg)
12500	NEDC	Fuzzy	0.5970
		On/Off	0.8893
	WLTP	Fuzzy	1.2460
		On/Off	1.3570
16000	NEDC	Fuzzy	0.6732
		On/Off	0.8893
	WLTP	Fuzzy	1.3820
		On/Off	1.3570
19500	NEDC	Fuzzy	0.7556
		On/Off	0.8893
	WLTP	Fuzzy	1.5240
		On/Off	1.3570

Table 6. Effects of aerodynamic drag coefficient on hydrogen consumption

Drag Coefficient (C_d)	Drive Cycle	Energy Technique	Hydrogen Consumed (kg)
0.60	NEDC	Fuzzy	0.5908
		On/Off	0.8893
	WLTP	Fuzzy	1.2310
		On/Off	1.3570
0.65	NEDC	Fuzzy	0.5970
		On/Off	0.8893
	WLTP	Fuzzy	1.2460
		On/Off	1.3570
0.70	NEDC	Fuzzy	0.6025
		On/Off	0.8893
	WLTP	Fuzzy	1.2610
		On/Off	1.3570

Table 7. Effects of rolling resistance coefficient on hydrogen consumption

Rolling Resistance Coefficient (Crr)	Drive Cycle	Energy Technique	Hydrogen Consumed (kg)
0.012	NEDC	Fuzzy	0.5673
		On/Off	0.8893
	WLTP	Fuzzy	1.1920
		On/Off	1.3570
0.015	NEDC	Fuzzy	0.5970
		On/Off	0.8893
	WLTP	Fuzzy	1.2460
		On/Off	1.3570
0.020	NEDC	Fuzzy	0.6449
		On/Off	0.8893
	WLTP	Fuzzy	1.3430
		On/Off	1.3570

Table 8. Effects of rolling resistance coefficient on hydrogen consumption

State of Regenerative Braking	Drive Cycle	Energy Technique	Vehicle Range (km)
On	NEDC	Fuzzy	492.02
		On/Off	448.85
	WLTP	Fuzzy	407.61
		On/Off	362.33
Off	NEDC	Fuzzy	455.40
		On/Off	400.40
	WLTP	Fuzzy	376.90
		On/Off	332.06

4. Conclusion

In this study, a PEM fuel cell electric bus which has two energy management techniques – traditional on-off and fuzzy logic – was created in MATLAB/Simulink. The performance of the bus under each of these energy management strategies was studied. Also, the consumption of hydrogen under different vehicle parameters including mass and resistance coefficients was investigated. Finally, the effects of regenerative braking on the total range of the bus were examined. It was observed that under the fuzzy logic energy management technique, the bus reaches relatively longer ranges with higher fuel cell efficiencies as compared to the on-off system. Also, increases in values of vehicle parameters like mass, drag coefficient and rolling resistance coefficient decreased the fuel cell efficiency increasing the rate of hydrogen consumption. Furthermore, the bus was able to reach longer ranges with regenerative braking. Future works can focus on comparing the fuzzy logic energy management strategy to more advanced energy control techniques such as reinforcement learning to further increase fuel cell efficiency and the range of PEM Fuel Cell Electric Vehicles.

Author's Declaration

Authors' contributions and responsibilities

The authors made substantial contributions to the conception and design of the study. The authors took responsibility for data analysis, interpretation and discussion of results. The authors read and approved the final manuscript.

Funding

No funding information from the authors.

Availability of data and materials

All data are available from the authors.

Competing interests

The authors declare no competing interest.

Additional information

No additional information from the authors.

Nomenclature

a	acceleration (m/s²)
A	active area of fuel cell (cm²)
A_f	frontal area of vehicle (m²)
B	constant that depends on the nature of the fuel cell and how it operates (V)
C_d	aerodynamic drag coefficient
C_{O_2}	concentration of oxygen (mol/cm³)
C_{rr}	coefficient of rolling resistance
CNG	compressed natural gas
E	energy of fuel cell (kWh)
F	Faraday's constant (C/mol)
F_{acc}	acceleration resistance (N)
F_d	aerodynamic resistance (N)
F_g	gradient resistance (N)
F_{roll}	rolling resistance (N)
F_{total}	total resistance force (N)
FC	fuel cell
FCEV	fuel cell electric vehicle
g	acceleration due to gravity (m/s²)
i_{diff}	gear ratio of differential
i_{FC}	operating current of fuel cell (A)
J	actual fuel cell current density (A/cm²)
J_{axle}	moment of inertia of axle (kgm²)
J_{max}	maximum fuel cell current density (A/cm²)
J_{total}	total moment of inertia (kgm²)
J_{wheel}	moment of inertia of wheel (kgm²)
J_n	current density when there is no load (A/cm²)
l	thickness of membrane (μm)
$\dot{m}_{H_2}$	flow of hydrogen (g/s)
$\dot{m}_{O_2}$	flow of oxygen (g/s)
m	mass of vehicle (kg)
M_{H_2}	mass of hydrogen (g/mol)
M_{motor}	torque of motor (Nm)
M_{net}	net motor torque (Nm)
M_{O_2}	mass of oxygen (g/mol)
M_{resis}	torque due to resistance forces (Nm)
$\dot{n}_{H_2}$	flow of hydrogen (mol/s)
$\dot{n}_{O_2}$	flow of oxygen (mol/s)
N	number of cells
NEDC	new european driving cycle
P_{FC}	fuel cell power (W)
P_{H_2}	pressure of hydrogen (atm)
P_{O_2}	pressure of oxygen (atm)

Nomenclature

PEM	proton exchange membrane
r_w	wheel radius (m)
R_C	contact resistance owing to electron flow (Ω)
R_m	membrane resistance due to the exchange of protons (Ω)
T	operating temperature of fuel cell (K)
T_{resis}	torque due to resistance forces (Nm)
V	vehicle velocity (m/s)
V_{stack}	voltage of fuel cell stack (V)
V_0	velocity of wind (m/s)
WLTP	worldwide harmonized light vehicle test procedure
ρ	density of air (kg/m³)
ρ_m	specific resistivity of membrane (Ωcm)
η_{diff}	efficiency of differential (%)
η_{FC}	efficiency of fuel cell (%)
η_{motor}	efficiency of motor (%)
$\xi_i (i = 1 \dots 4)$	adjustable parametric coefficients of cell model
ΔH	enthalpy change for fuel cell reaction (kJ/mol)
ψ	adjustable parametric coefficient of cell model
θ	angle of slope
ω	angular velocity (rad/s)

References

[1] Q. Hassan, I. D. J. Azzawi, A. Z. Sameen, and H. M. Salman, "Hydrogen Fuel Cell Vehicles: Opportunities and Challenges," *Sustainability*, vol. 15, no. 15, p. 11501, Jul. 2023, doi: 10.3390/su151511501.

[2] G. W. Crabtree and M. S. Dresselhaus, "The Hydrogen Fuel Alternative," *MRS Bulletin*, vol. 33, no. 4, pp. 421–428, Apr. 2008, doi: 10.1557/mrs2008.84.

[3] B. Tanç, H. T. Arat, E. Baltacıoğlu, and K. Aydın, "Overview of the next quarter century vision of hydrogen fuel cell electric vehicles," *International Journal of Hydrogen Energy*, vol. 44, no. 20, pp. 10120–10128, Apr. 2019, doi: 10.1016/j.ijhydene.2018.10.112.

[4] I. C. Setiawan and M. Setiyo, "Fueling the Future: The Case for Heavy-Duty Fuel Cell Electric Vehicles in Sustainable Transportation," *Automotive Experiences*, vol. 7, no. 1, pp. 1–5, Apr. 2024, doi: 10.31603/ae.11285.

[5] M. Setiyo, "Sustainable Transport: The Role of Clean Energy, Mass Rapid Transit, Non-motorized Mobility, and Challenges to Achievement," *Automotive Experiences*, vol. 6, no. 1, pp. 1–3, 2023, doi: 10.31603/ae.9108.

[6] I. Abdullaev, N. Lin, and J. Rashidov, "Electric Vehicles: Manuscript of a Bibliometric Analysis Unveiling Trends, Innovations and Future Pathways," *International Journal of Automotive Science And Technology*, vol. 8, no. 2, pp. 212–224, Jun. 2024, doi: 10.30939/ijastech..1424879.

[7] M. N. K. Jarkoni *et al.*, "Effects of exhaust emissions from diesel engine applications on environment and health: A review," *Journal of Sustainability Science and Management*, vol. 17, no. 1, pp. 281–301, Jan. 2022, doi: 10.46754/jssm.2022.01.019.

[8] A. A. Abdel-Rahman, "On the emission from internal combustion engines: A review," *International Journal of Energy Research*, vol. 22, no. 6, pp. 483–513, 1998, doi: 10.1002/(SICI)1099-114X(199805)22:6<483::AID-ER377>3.0.CO;2-ZCITATIONS145.

[9] S. K. Ankathi, J. Bouchard, and X. He, "Beyond Tailpipe Emissions: Life Cycle Assessment Unravels Battery's Carbon Footprint in Electric Vehicles," *World Electric Vehicle Journal*, vol. 15, no. 6, p. 245, Jun. 2024, doi: 10.3390/wevj15060245.

[10] J. A. Sanguesa, V. Torres-Sanz, P. Garrido, F. J. Martinez, and J. M. Marquez-Barja, "A Review on Electric Vehicles: Technologies and Challenges," *Smart Cities*, vol. 4, no. 1, pp. 372–404, Mar. 2021, doi: 10.3390/smartcities4010022.

[11] C. E. Thomas, "Fuel cell and battery electric vehicles compared," *International Journal of Hydrogen Energy*, vol. 34, no. 15, pp. 6005–6020, Aug. 2009, doi: 10.1016/j.ijhydene.2009.06.003.

[12] E. Schaltz, "Electrical Vehicle Design and Modeling," in *Electric Vehicles - Modelling and Simulations*, InTech, 2011. doi: 10.5772/20271.

[13] A. O. Kiyakli and H. Solmaz, "Modeling of an Electric Vehicle with MATLAB/Simulink," *International Journal of Automotive Science and Technology*, vol. 2, no. 4, pp. 9–15, Dec. 2018, doi: 10.30939/ijastech..475477.

[14] T. Kocakulak, V. K. T. Thallapalli, and A. O. Kiyakli, "Modeling of an Electric Tractor and Determining Energy Consumption Values In Different Duties," *Engineering Perspective*, vol. 2, no. 2, pp. 79–85, 2021, doi: 10.29228/eng.pers.51651.

[15] O. Karakaş, U. B. Şeker, and H. Solmaz, "Modeling of an Electric Bus Using

MATLAB/Simulink and Determining Cost Saving for a Realistic City Bus Line Driving Cycle," *Engineering Perspective*, vol. 2, no. 2, pp. 52–62, 2021, doi: 10.29228/eng.pers.51422.

[16] H. Hemi, J. Ghouili, and A. Cheriti, "A real time fuzzy logic power management strategy for a fuel cell vehicle," *Energy Conversion and Management*, vol. 80, pp. 63–70, Apr. 2014, doi: 10.1016/j.enconman.2013.12.040.

[17] N. Mebarki, T. Rekioua, Z. Mokrani, D. Rekioua, and S. Bacha, "PEM fuel cell/ battery storage system supplying electric vehicle," *International Journal of Hydrogen Energy*, vol. 41, no. 45, pp. 20993–21005, Dec. 2016, doi: 10.1016/j.ijhydene.2016.05.208.

[18] Dana TM4, "TM4 Sumo HD," *Dana TM4*, 2024. https://www.danatm4.com/products/systems/sumo-hd/ (accessed Mar. 01, 2024).

[19] G. Hwang, K. Lee, J. Kim, K.-J. Lee, S. Lee, and M. Kim, "Energy Management Optimization of Series Hybrid Electric Bus Using an Ultra-Capacitor and Novel Efficiency Improvement Factors," *Sustainability*, vol. 12, no. 18, p. 7354, Sep. 2020, doi: 10.3390/su12187354.

[20] M. Ehsani, Y. Gao, S. Longo, and K. M. Ebrahimi, *Modern electric, hybrid electric, and fuel cell vehicles*, 3rd ed. CRC Press, 2018.

[21] S. Çetinkaya, *Taşıt Mekaniği*. Nobel Akademik Yayıncılık, 2023.

[22] T. K.-E. Yurdaer, "Comparison of Energy Consumption of Different Electric Vehicle Power Systems Using Fuzzy Logic-Based Regenerative Braking," *Engineering Perspective*, vol. 1, no. 1, pp. 11–21, 2021, doi: 10.29228/sciperspective.47590.

[23] A. O. Kiyakli, "6x6 Seri hibrit elektrikli bir zirhli personel taşıyıcının modellenmesi," Gazi University, 2022.

[24] T. Kocakulak and H. Solmaz, "Ön ve son iletimli paralel hibrit araçların bulanık mantık yöntemi ile kontrolü ve diğer güç sistemleri ile karşılaştırılması," *Gazi Üniversitesi Mühendislik Mimarlık Fakültesi Dergisi*, vol. 35, no. 4, pp. 2269–2286, Jul. 2020, doi: 10.17341/gazimmfd.709101.

[25] Xiaohong Nian, Fei Peng, and Hang Zhang, "Regenerative Braking System of Electric Vehicle Driven by Brushless DC Motor," *IEEE Transactions on Industrial Electronics*, vol. 61, no. 10, pp. 5798–5808, Oct. 2014, doi: 10.1109/TIE.2014.2300059.

[26] J. M. Correa, F. A. Farret, L. N. Canha, and M. G. Simoes, "An Electrochemical-Based Fuel-Cell Model Suitable for Electrical Engineering Automation Approach," *IEEE Transactions on Industrial Electronics*, vol. 51, no. 5, pp. 1103–1112, Oct. 2004, doi: 10.1109/TIE.2004.834972.

[27] J. M. Correa, F. A. Farret, V. A. Popov, and M. G. Simoes, "Sensitivity Analysis of the Modeling Parameters Used in Simulation of Proton Exchange Membrane Fuel Cells," *IEEE Transactions on Energy Conversion*, vol. 20, no. 1, pp. 211–218, Mar. 2005, doi: 10.1109/TEC.2004.842382.

[28] G. N. Srinivasulu, T. Subrahmanyam, and V. D. Rao, "RETRACTED: Parametric sensitivity analysis of PEM fuel cell electrochemical Model," *International Journal of Hydrogen Energy*, vol. 36, no. 22, pp. 14838–14844, Nov. 2011, doi: 10.1016/j.ijhydene.2011.03.040.

[29] A. S. Menesy, H. M. Sultan, A. Korashy, F. A. Banakhr, M. G. Ashmawy, and S. Kamel, "Effective Parameter Extraction of Different Polymer Electrolyte Membrane Fuel Cell Stack Models Using a Modified Artificial Ecosystem Optimization Algorithm," *IEEE Access*, vol. 8, pp. 31892–31909, 2020, doi: 10.1109/ACCESS.2020.2973351.

[30] F. Barbir, *PEM fuel cells: Theory and Practice.* Academic Press, 2012.

[31] J. Zhang, J. Wu, and H. Zhang, *PEM Fuel cell testing and diagnosis*. Newnes, 2013.

[32] Y. D. Herlambang *et al.*, "Application of a PEM Fuel Cell Engine as a Small-Scale Power Generator for Small Cars with Different Fuel Concentrations," *Automotive Experiences*, vol. 6, no. 2, pp. 273–289, Aug. 2023, doi: 10.31603/ae.9225.

[33] G. Sefkat and M. A. Özel, "Pem Yakit Pilinin Simulink Modeli ve Analizi," *Uludağ University Journal of The Faculty of Engineering*, vol. 23, no. 2, pp. 351–366, Oct. 2018, doi: 10.17482/uumfd.400337.

[34] N. M. Boyacioğlu, T. Kocakulak, M. Batar, A. Uyumaz, and H. Solmaz, "Modeling and Control of a PEM Fuel Cell Hybrid Energy System Used in a Vehicle with Fuzzy Logic Method," *International Journal of Automotive*

Science and Technology, vol. 7, no. 4, pp. 295–308, Dec. 2023, doi: 10.30939/ijastech..1340339.

[35] S. N. Sivanandam, S. Sumathi, and S. N. Deepa, *Introduction to Fuzzy Logic using MATLAB*. Berlin, Heidelberg: Springer Berlin Heidelberg, 2007. doi: 10.1007/978-3-540-35781-0.

[36] N. Sulaiman, M. A. Hannan, A. Mohamed, E. H. Majlan, and W. R. Wan Daud, "A review on energy management system for fuel cell hybrid electric vehicle: Issues and challenges," *Renewable and Sustainable Energy Reviews*, vol. 52, pp. 802–814, Dec. 2015, doi: 10.1016/j.rser.2015.07.132.

[37] M. Ö. Yatak, Ç. Hisar, and F. Şahin, "Fuzzy Logic Controller for Half Vehicle Active Suspension System: An Assessment on Ride Comfort and Road Holding," *International Journal of Automotive Science And Technology*, vol. 8, no. 2, pp. 179–187, 2024, doi: 10.30939/ijastech..1372001.

[38] İ. Özmen and C. Közkurt, "Design of Fuzzy Logic Supported Car Driver Control System," *International Journal of Automotive Science and Technology*, vol. 5, no. 3, pp. 228–238, Sep. 2021, doi: 10.30939/ijastech..902139.

[39] T. Alp Arslan, F. E. Aysal, İ. ÇELİK, H. Bayrakçeken, and T. N. Öztürk, "Quarter Car Active Suspension System Control Using Fuzzy Controller," *Engineering Perspective*, vol. 4, no. 4, pp. 33–39, 2022, doi: 10.29228/eng.pers.66798.

[40] A. Kabza, *Just another Fuel Cell Formulary*. 2022. [Online]. Available: https://www.kabza.de/pemfc.de/FCF_A4.pdf

[41] J. Larminie and A. Dicks, *Fuel cell systems explained*. Wiley-Blackwell, 2003.